J. Biochem. 2012;151(6):633–642 doi:10.1093/jb/mvs045

JB THE JOURNAL OF BIOCHEMISTRY

Deuterium kinetic isotope effects in heterotetrameric sarcosine oxidase from *Corynebacterium* sp. U-96: the anionic form of the substrate in the enzyme–substrate complex is a reactive species

Received November 30, 2011; accepted February 16, 2012; published online April 23, 2012

Mutsumi Saito[1], Ai Itoh[2] and Haruo Suzuki[1,2,*]

[1]Division of Bioscience, Graduate School of Basic Life Science and [2]Department of Biosciences, School of Science, Kitasato University, Kitasato 1-15-1, Sagamihara-shi, Kanagawa-ken 252-0329, Japan

*Haruo Suzuki, School of Science, Kitasato University, Kitasato 1-15-1, Sagamihara-shi, Kanagawa-ken 252-0329, Japan. Tel:/Fax: +81-42-741-5526, email: suzukih@kitasato-u.ac.jp

Heterotetrameric sarcosine oxidase is a flavoprotein that catalyses the oxidative demethylation of sarcosine. It is thought that the dehydrogenated substrate is the anionic form of sarcosine. To verify this assumption, the rate of flavin-adenine dinucleotide (FAD) reduction (k_{red}) was analysed using protiated and deuterated sarcosine (*N*-methyl-d_3-Gly) at various pH values using stopped-flow method. By increasing the pH from 6.2 to 9.8, k_{red} increased for both substrates and reached a plateau, but the pK_a value (reflecting the ionization of the enzyme–substrate complex) was 6.8 and 7.1 for protiated and deuterated sarcosine, respectively, and the kinetic isotope effect of k_{red} decreased from approximately 19 to 8, indicating deprotonation of the bound sarcosine. The k_{red}/K_d (K_d, sarcosine dissociation constant) increased with increasing pH and reached a plateau. The pK (reflecting the ionization of free enzyme or free sarcosine) was 7.0 for both substrates, suggesting deprotonation of the βLys358 residue, which has a pK_a of 6.7, as the pK_a of the free sarcosine amine proton was determined to be approximately 10.1. These results indicate that the amine proton of sarcosine is transferred to the unprotonated Lys residue in the enzyme–substrate complex.

Keywords: substrate dehydrogenation/heterotetrameric sarcosine oxidase/kinetic isotope effect/low pK_a Lys/substrate ionization.

Abbreviations: D-Sar, deuterated sarcosine; Eox, the oxidized form of enzyme; Ered, the reduced form of enzyme; H-Sar, protiated sarcosine; MSO, monomeric sarcosine oxidase; MTA, methylthioacetate; SO, heterotetrameric sarcosine oxidase; SO-U96, SO from *Corynebacterium* sp. U96; THF, tetrahydrofolate.

Heterotetrameric sarcosine oxidase [SO; sarcosine: oxygen oxidoreductase (demethylating), EC 1.5.3.1] catalyses the oxidative demethylation of sarcosine to generate glycine, hydrogen peroxide and formaldehyde or 5,10-methylenetetrahydrofolate (5, 10-CH_2-THF), depending on the availability of tetrahydrofolte (THF) (*1*) (Scheme 1). SO from *Corynebacterium* sp. U96 (SO-U96) comprises four non-identical subunits (α, 110 kDa; β, 44 kDa; γ, 21 kDa; δ, 10 kDa) and one non-covalently bound flavin-adenine dinucleotide (FAD), one covalently bound flavin mononucleotide (FMN) and one NAD^+ (*1*, *2*). Non-covalent FAD is reduced by sarcosine and electrons are transferred from the reduced FAD to covalent FMN. The reduced FMN is oxidized by molecular oxygen to yield the oxidized flavin cofactors (*3*). These properties of SO are common among reported SOs (*1*,*3*–*5*). Recombinant SO-U96 is expressed with high yield in *Escherichia coli* and retains the catalytic properties of the native enzyme (*6*). The enzyme has been crystallized, and the 3D structure was constructed based on X-ray crystallography (*7*).

The pK_a values of the carboxylate and the secondary amine of sarcosine are 2.23 and 10.01, respectively (*5*). Therefore, sarcosine exists in the zwitterionic form in the neutral pH region. However, the anionic form of sarcosine has been assumed to react with oxidized FAD in the active site of SOs from *Corynebacterum* sp. U-96, *C.* sp. P1 and *Arthrobacter* sp. 1-IN (*4*, *5*, *8*, *9*). The 3D structure of SO-U96 revealed that the carboxylate group of the substrate analogue methylthioacetate (MTA) is bound to the side chains of the Lys358 and Arg59 residues of the β-chain in SO-U96 (*10*) but that the other residues surrounding the analogue are hydrophobic. Therefore, to accommodate the hydrophobic nature of the active site, we postulated that the bound sarcosine is deprotonated at the active site (*10*). These assumptions seem to be reasonable, but clear evidence is necessary. Trimethylamine dehydrogenase (TMADH) and monomeric sarcosine oxidase (MSO) have been used to examine the ionization state of substrates in the enzyme–substrate complex. On the basis of the observation that deuteration of the atoms bonded to the amine nitrogen causes an increase in the amine pK_a (*11*–*13*), Basran *et al.* (*14*) demonstrated substrate ionization of TMADH. The anaerobic flavin reduction of TMADH using trimethylamine (TMA) is controlled by a single macroscopic ionization (pK_a 6.8), but this ionization is perturbed (pK_a 7.4) when perdeuterated TMA is used (*11*). The observed macroscopic ionization was attributed to the ionization of the amine proton rather than that of groups on the enzyme. Dunn *et al.* applied this method to monoamine oxidase A (MAO A) (*15*) and suggested that the neutral amine is stabilized in the MAO A–substrate complex. Using a different approach, Zhao and Jorns (16–18) showed that the unprotonated form of substrate is the reactive species in the MSO-catalysed reaction. The pH dependence of the

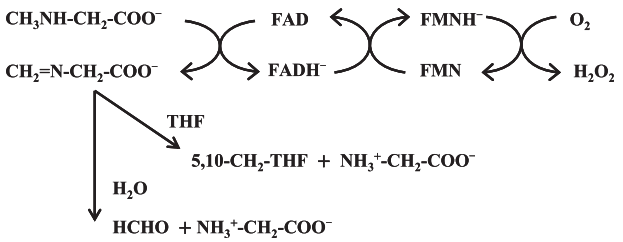

Scheme 1 Oxidation of sarcosine by SO in the presence and absence of THF.

maximum rate of the reductive half-reaction with L-Pro as substrate indicates that the ionizable group in the MSO–L-Pro complex is unprotonated during conversion to the MSO–product complex (pK_a 8.02) (*16*). The oxidized form of MSO forms a charge–transfer complex with L-Pro (pK_a 7.94), and the charge–transfer interaction with L-Pro as a donor and FAD as an acceptor is possible only when L-Pro is in the anionic form (*16*). Therefore, the anionic form of L-Pro in the MSO–L-Pro complex is the reactive species (*16*, *17*). These conclusions were confirmed by analysis of the MSO-catalysed oxidation of sarcosine (*18*). The active site of SOs is reported to be hydrophobic (*10*, *19*) but that of MSO is composed of hydrophilic residues such as His (*20*). The difference in the active site structure of MSO and SOs led us to study the ionization state of sarcosine in the SO-U96-catalysed reaction. In this study, we applied the method reported for the TMADH-catalysed reaction (*14*) and showed that the anionic form of sarcosine is the active species in the enzymatic reaction.

Materials and Methods

Materials

Protiated sarcosine (H-Sar, *N*-methylglycine HCl) was obtained from Wako Chemicals (Osaka, Japan) and deuterated sarcosine (D-Sar; *N*-methyl-d_3-glycine HCl, 99 atom % deuterium) from C/D/N Isotopes (Quebec, Canada). Stock sarcosine solution was prepared by neutralizing with potassium hydroxide solution.

Spectroscopy

Absorption spectra were measured using a double-beam spectrophotometer (Ubest-50, Japan Spectroscopic, Tokyo, Japan).

Steady-state rate measurements

Enzyme activity was assayed by measuring oxygen uptake using an oxygen electrode (Strathkelvin Instruments, North Lanarkshire, Scotland) in the presence of various concentrations of sarcosine in 50 mM buffer containing 100 mM KCl at 25°C. Buffers used included potassium phosphate (pH 5.8–7.9), sodium pyrophosphate (pH 7.9–9.5) and sodium borate (pH 9.5–10.5). After each measurement, the pH of the reaction mixture was measured, and this value was used to analyse the results. Oxygen concentration in the buffer was assumed to be 256 μM at 25°C. The reaction rate (v/e) was expressed as the molar concentration of oxygen consumed per second per molar concentration of enzyme, and k_{cat} was the rate at the limiting concentration of sarcosine. The concentration (e) of enzyme was determined by measuring the amount of enzyme-bound flavins, assuming that the extinction co-efficient of the enzyme-bound flavin is 11.3 $mM^{-1}cm^{-1}$ at 450 nm. The 'e' value is half of the flavin concentration as the enzyme contains two flavins per molecule.

Stopped-flow spectroscopy

Rapid reaction kinetic experiments were performed using a 3×17 MV stopped-flow spectrophotometer (Applied Photophysics, Surrey, UK) equipped with a HAAKE temperature controller as described previously (*9*). Buffers used were the same as those described for steady-state rate measurements. Experiments were performed in the presence of 40 mM sodium sulphite because sulphite binds specifically to the FMN cofactor of the enzyme to inhibit flavin reduction (*4*, *9*). Time-dependent spectral or absorbance changes were monitored using a photodiode array detector or single wavelength detector, respectively. In single wavelength studies, FAD reduction with sarcosine was observed at 450 nm. The time course of the absorbance change at a single wavelength was fit to a single exponential process using software connected to the apparatus. The equation used for analyses was as follows:

$$A_{450} = C\exp.(-k_{obs}t) + b$$

where C is the relative amplitude value for the fast phase and b is an offset value to account for a non-zero baseline.

Analyses of rates versus pH

Maximum rates of the steady-state reaction (k_{cat}) and of the reductive half-reaction ($k_{red/max}$) of the enzyme-bound FAD at various pH levels were determined at the limiting concentration of sarcosine and analysed using the following equations:

$$k_{obs} = \frac{k_{ind}}{1 + [H^+]/K_{a1} + K_{a2}/[H^+]} \quad (1)$$

$$k_{obs}/K_{obs} = \frac{k_{ind}/K_{ind}}{1 + [H^+]/K_1 + K_2/[H^+]} \quad (2)$$

where k_{obs} represents the maximum rates obtained at various pH values, and k_{ind} is the pH-independent maximum rate. K_{obs} is the dissociation constant (or Michaelis constant) of the substrate at various pH values, and K_{ind} is the pH-independent dissociation constant (or Michaelis constant) of the substrate. K_{a1} and K_{a2} are dissociation constants for the ionizable group of the enzyme–substrate complex, and K_1 and K_2 are those of ionizable groups for the enzyme or substrate sarcosine.

Results

pH dependence of steady-state rates

SO-U96 has an apparent K_m of ~20 μM for oxygen (*4*, *9*); therefore, kinetic parameters obtained using air-saturated buffer are expected to reflect the reductive half-reaction of the enzyme with sarcosine. The k_{cat} values exhibited bell-shaped pH dependence, indicating the presence of two ionizable groups in the EoxS complex, which have pK_a values of 6.7 ± 0.1 and 10.1 ± 0.2, respectively, based on curve fitting (Fig. 1A). Here, Eox and S represent the oxidized forms of the enzyme and substrate, respectively. The results indicate that, with increasing pH, a group in the EoxS complex is deprotonated for optimal activity, followed by deprotonation of the second group to diminish this activity. The k_{cat}/K_m values also exhibit bell-shaped pH dependence, indicating the presence of two ionizable groups in the free enzyme or in sarcosine, which have pK_a values of 7.4 ± 0.1 and 9.8 ± 0.2, respectively, based on curve fitting (Fig. 1B). Thus, increasing the pH deprotonates a group in the free enzyme or substrate, inducing optimal enzyme activity, followed by deprotonation of the second group to diminish this activity. These results suggest that ionizable groups in the EoxS complex and in the free enzyme or the free substrate are required for optimal activity, and the present results indicate that the ionizable groups are involved in the reductive steps.

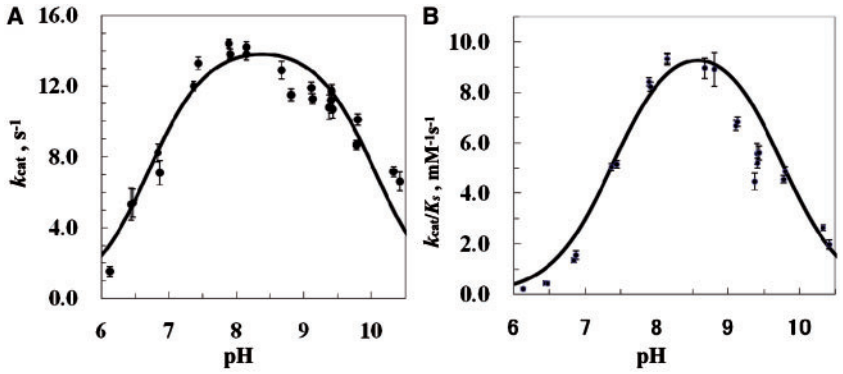

Fig. 1 Effect of pH on the steady-state kinetic parameters of the SO-U96-catalysed reaction. (A) k_{cat} values obtained at the limiting concentration of H-Sar (filled circle) were fitted with $pK_a = 6.7$ and $pK_b = 10.1$, and $k_{ind} = 14.4\,s^{-1}$ (line). (B) k_{cat}/K_m values for H-Sar were fitted with $pK_1 = 7.4$ and $pK_2 = 9.8$, and $k_{ind}/K_{ind} = 9.75$ (line).

However, the mechanism of the reductive half-reaction is complex (*4*, *9*); after EoxS complex formation, reduction of the bound FAD cofactor occurs, the electron transfers from the reduced FAD to the bound FMN cofactor, then the oxidized FAD is reduced again following EoxS complex formation. Thus, it is difficult to identify in which step the ionizable group(s) is (are) involved. To simplify the analysis, we measured FAD reduction using the stopped-flow method in the presence of sodium sulphite.

Analyses of FAD cofactor reduction with sarcosine

The covalently bound FMN specifically binds with sulphite to form the FMN-sulphite adduct in SOs, thus inhibiting reduction of FMN by the reduced FAD cofactor (*4*, *9*). We examined the reduction process of FAD in the presence of sulphite by monitoring the flavin spectrum during reduction with sarcosine at three different pH values. Figure 2 shows the photodiode array spectral change at various pH values. At approximately pH 6 and 8, spectral changes after addition of sarcosine were similar to those reported for wild-type SO-U96 (*9*); the formation of spectrum with a shoulder at ~410 nm was observed, which was accompanied by a slow decrease of the shoulder. At approximately pH 10, the flavin spectrum was observed after a fast spectral change and then gradually changed to the fully reduced spectrum using H-Sar and D-Sar (Fig. 2C and F), although a spectrum with a longer incubation time is not shown for D-Sar (Fig. 2F). The spectral change using D-Sar was slow at approximately pH 10, but nearly complete reduction of flavin cofactors was observed after incubation for 888 s. Comparing the total absorbance change of flavin at 450 nm (~0.07) at alkaline pH with those at approximately pH 6 and 8 (~0.04), the change at alkaline pH is nearly twice that at the other pH values. This suggests that sarcosine reduces both FAD and FMN cofactors even in the presence of sodium sulphite, but that FMN reduction is very slow compared with FAD reduction. This means that sulphite is loosely bound to the enzyme FMN at approximately pH 10. The idea is supported by a study reporting that the dissociation constant of the sulphite adduct of D-amino acid oxidase is relatively large at acidic and alkaline pH values (*21*), although we did not determine the dissociation constant of the SO-U96–sulphite complex at these pH values. At approximately pH 10, fast and slow phases are clearly observed (Fig. 2), and we therefore assumed that the fast stage represents the reduction of enzyme-bound FAD.

As described earlier, flavin reduction in the presence of 40 mM sulphite at different pH values represents reduction of the FAD cofactor, thus the absorbance change at 450 nm was monitored using the stopped-flow method at 25°C. The initial fast changes in absorbance at three different pH values were fitted to single exponential process with both H-Sar and D-Sar but did not fit well for H-Sar at pH 6.1 and 9.7 (Fig. 3). The rate (k_{red}) of reduction at various concentrations of sarcosine was determined using Equation (3):

$$k_{red} = k_{red/max}\frac{[Sar]}{K_d + [Sar]} \quad (3)$$

where $k_{red/max}$, K_d and Sar represent the maximum rate of reduction obtained at the limiting concentration of sarcosine, the dissociation constant of the enzyme–sarcosine complex and sarcosine, respectively. The $k_{red/max}$ values were plotted against pH (Fig. 4A). From the plot, the pK_a value (6.8 ± 0.2) determined using H-Sar is clearly different from that determined using D-Sar ($pKa = 7.1 \pm 0.1$). To more clearly show the pK difference, the kinetic isotope effect (KIE) was determined and plotted (Fig. 4C). KIE was strongly dependent on pH. Values agreed well with the KIE values calculated using Equation (1).

The $k_{red/max}/K_d$ values increased with increasing pH and reached a plateau (Fig. 4B). The pK value reflects the ionization of the kinetically important group on the free enzyme or free substrate and was determined to be 7.0 ± 0.1 based on curve fitting with H-Sar and D-Sar (Fig. 4B). The deuterium isotope effect on $k_{red/max}/K_d$ was plotted against pH, which agreed well with the calculated value (Fig. 4D). The pK values obtained are summarized in Table 1.

Discussion

The pK_a values of 6.8 and 7.1 were determined from the pH profile of the rate of FAD reduction with H-Sar

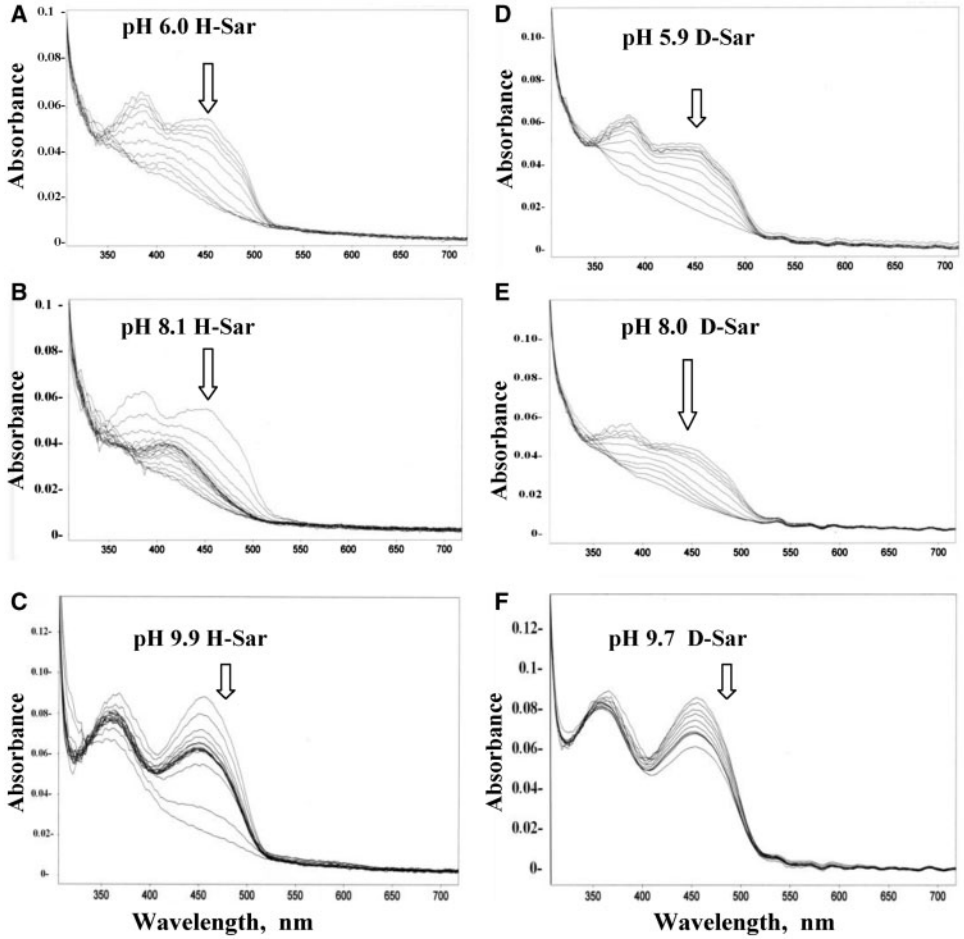

Fig. 2 Photodiode array spectral change with time at various pH values in the presence of 40 mM sodium sulphite at 25°C. Spectra were acquired every 25.6 ms from 1.28 ms (top) to 5.36 s (bottom) in (A) and every 15.36 ms from 1.28 ms (top) to 8.12 s (bottom) in (B) and (C). Spectra were obtained every 0.57 s from 0 s (top) to 5.2 s (bottom) in (D–F). After incubation for 888 s with D-Sar at pH 9.7, a spectrum similar to that obtained after incubation for 8.12 s with H-Sar (C) was observed, although this is not shown in (F). The final concentrations of enzyme and sarcosine were 5 μM and 5 mM, respectively. Arrow indicates the direction of absorbance change.

and D-Sar, respectively (Fig. 4A). The KIE decreased from approximately 19 to approximately 7 as pH increased (Fig. 4C). The pK_a value reflects the deprotonation of the ionisable group in the enzyme–substrate complex. The protonated secondary amine group of sarcosine has pK_a values of 10.05 ± 0.05 and 10.16 ± 0.04 for H-Sar and D-Sar, respectively (Supplementary Table S1). These results support the hypothesis that deuteration of atoms bonded to the amine nitrogen causes an increase in the amine pK_a (*11–13*). The higher KIE of FAD reduction at lower pH values (Fig. 4C) supports the idea that ionization in the enzyme–substrate complex is due to deprotonation of sarcosine. The elevated pK_a values observed with D-Sar results in a higher concentration of $EoxH^+SH^+$ (inactive) than $EoxH^+S$ (active) (Scheme 2A), thus leading to a higher KIE at lower pH values (*5*, *11*, *15*). On the basis of these results, we propose that the ionisable group is the protonated sarcosine in the $EoxH^+SH^+$ complex and that sarcosine is dehydrogenated in the anionic form ($CH_3NH–COO^-$). The $k_{red/max}$ value for SO of *Arthrobacter* sp. 1-IN was reported to be pH independent (*5*). The difference in the value for the *Arthrobacter* enzyme and that determined in this study is due to an error in k_{red} determination as a large error was reported at pH 6.5 and 6.75 for the *Arthrobacter* enzyme (*5*). Fortunately, we were able to obtain rate data and determine the pK_a value, although the absorbance traces at pH 6.1 and 9.7 were relatively poor for H-Sar (Fig. 3A and C).

The pK_a value of bound sarcosine showed an acidic shift of 3.1–3.3 pH units compared with that of unbound sarcosine. An acidic pK_a shift has been observed for other enzymes, including TMADH ($\Delta pK_a \sim 3.5$) (*11*), MSO (ΔpK_a 2.6) (*17*) and mouse polyamine oxidase (ΔpK_a 0.8) (*22*). The ionization of amino acid residues in the active site is affected by the microenvironment surrounding the residues (*23*). For example, when the buried Val66 in the hydrophobic core of staphylococcal nuclease was replaced with either Lys or Glu, the pK_a value of Lys66 decreased by 4.9 pH units compared with the Lys residue in the denatured state (*24*) and that of Glu increased by 4.3 pH units compared with that of Glu in water (*25*). It is conceivable that the acidic pK_a shift of the amine proton of sarcosine is derived from the hydrophobic nature of the sarcosine-binding site (*10*). The pK_a difference between D-Sar and H-Sar is approximately

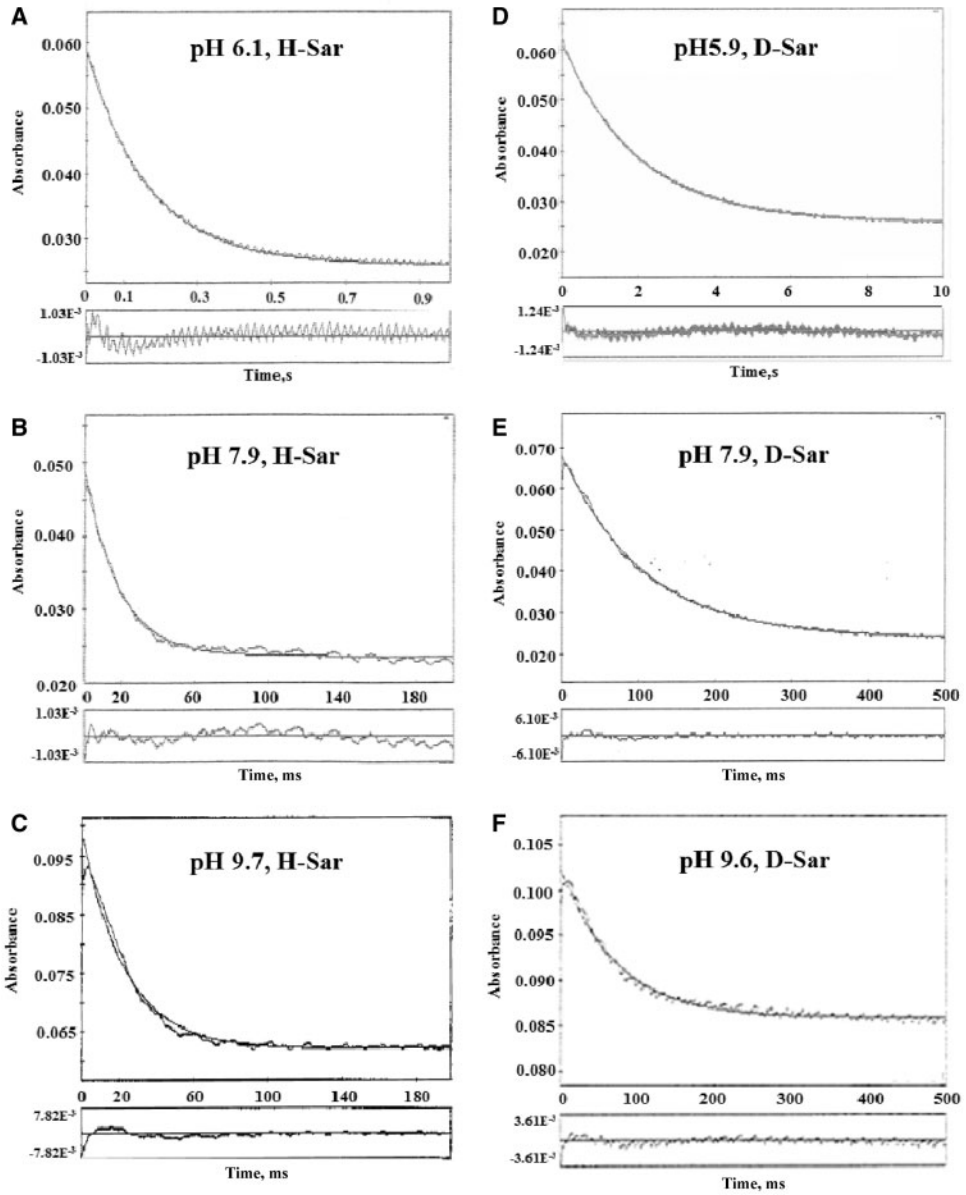

Fig. 3 Stopped-flow traces at 450 nm after mixing SO-U96 with H-Sar (A–C) or D-Sar (D–F). Conditions (after mixing); 5 μM enzyme, 10 mM sarcosine, 40 mM sulphite, ~pH 6.0 (A and D), pH 8.0 (B and E), pH 9.6 (C and F) at 25°C. The thick lines represent the data points, and the smooth thin lines are the single exponential fit to the data points.

0.1 in water, but the difference when these molecules were bound to SO-U96 was determined to be 0.3. The reason for this difference is not clear. However, the interaction of D-Sar with the active site residues might be different from that of H-Sar, and these different interactions may have induced an increase in the pK_a difference by binding with the enzyme. This idea is supported by the report on TMA dehydrogease (*14*, *26*). The pK_a of TMA is 9.8 for the protiated amine [$(CH_3)_3N$–H] and 10.1 for the deuterated amine [$(CD_3)_3$–NH] (ΔpK_a 0.3) (*14*), but those of the bound TMA in active site mutants have been reported to show acidic shifts of 0.8–3.6 pH units, and the ΔpK_a (deuteated minus protiated) is 0.6 for H172Q, 1.1 for Y60F and 0.8 for Y60F/H172Q mutants (*26*).

The active site structure (*9*, *10*) supports the proposal that the anionic form of sarcosine is the substrate for dehydrogenation. The ionisable groups in the β-subunit of the active site are Arg69, Lys358 and Tyr271. The pK_a of the ε-amino group of Lys358 was reported to be 6.7 (*27*), which agrees with the pK_a value of 6.8 obtained in this study (Fig. 4A); thus, the ε-amino group may be a candidate for the ionisable group. However, it is unlikely that this is the case. The structure of SO-U96 suggests that the carboxylate group of sarcosine is bound to the side chains of the Lys358 and Arg69 residues, and it is not conceivable that the pK_a of the ε-amino group of Lys358 is affected by deuteration of the methyl group of sarcosine. Moreover, ionization of Tyr271 is not related to the group having a pK_a of 6.8 as the

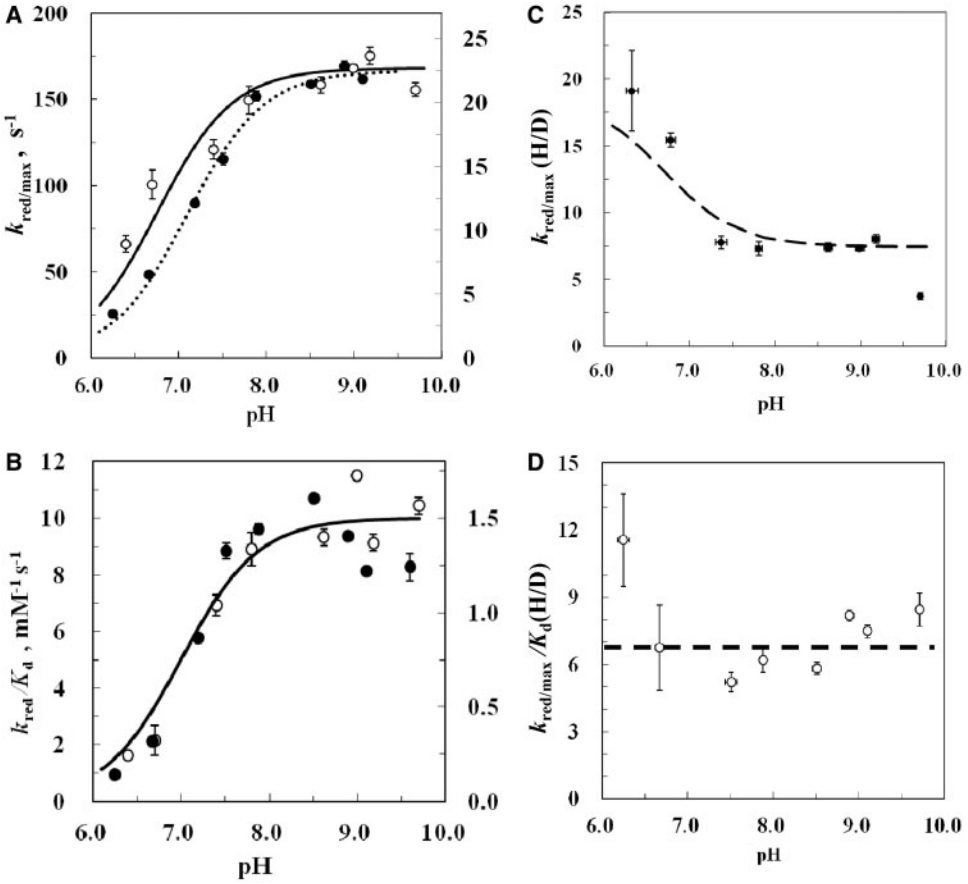

Fig. 4 Stopped-flow kinetic parameters versus pH. (A) The maximum rate ($k_{red/max}$) of FAD reduction of enzyme was determined at various pH from the traces shown in Fig. 3 and plotted against pH. Open circle, H-Sar (left axis); closed circle, D-Sar (right axis). Lines are fitted with pK 6.8 and $k_{red/max/ind}$ 168 s^{-1} for the data obtained for H-Sar and with pK 7.1 and $k_{red/max/ind}$ 22.5 s^{-1} for D-Sar at optimal pH. The $k_{red/max}$ of $34.6 \pm 1.9\,s^{-1}$ obtained with D-Sar at pH 9.6 is not shown in the plot. (B) $k_{red/max}/K_d$ values were plotted against pH. Lines are fitted with pK 7.0 for the data obtained with H-Sar (open circle, left axis) and D-Sar (closed circle, right axis), and $k_{red/max/ind}/K_{d/ind}$ values were 10 and 1.5 for H-Sar and D-Sar, respectively. (C) Kinetic isotope effects versus pH. The dashed line represents the theoretical values obtained assuming that the pH independent maximum rates are as in (A), and pK 6.8 and pK 7.1 are for H-Sar and D-Sar, respectively. (D) Deuterium isotope effect for $k_{red/max}/K_d$ versus pH. The dashed line represents the theoretical values (6.7) obtained by assuming the $k_{red/max/ind}/K_{d/ind}$ values used in (B) and using pK value of 7.0.

Table I. pK values obtained from curve-fitting for SO-U96 at 25°C.

		EoxS complex		Free Eox or S	
Substrates	**Methods**	**pK_{a1}**	**pK_{a2}**	**pK_1**	**pK_2**
H-Sar	Steady state	6.7 ± 0.1	10.1 ± 0.1	7.4 ± 0.1	9.8 ± 0.2
H-Sar	Stopped flow	6.8 ± 0.2		7.0 ± 0.1	
D-Sar	Stopped flow	7.1 ± 0.1		7.0 ± 0.1	

Tyr271Phe mutant of SO-U96, which does not have an ionisable hydroxyl group on Tyr271, showed a pH-dependent rate profile similar to that shown in Fig. 1A (*10*). If the ionization of Tyr271 is related to the group having a pK_a of 6.8, the Tyr271Phe mutant of SO-U96 should not show a pH-dependent rate profile. These observations strongly indicate that the group with a pK_a of 6.8 is the secondary amine group of sarcosine.

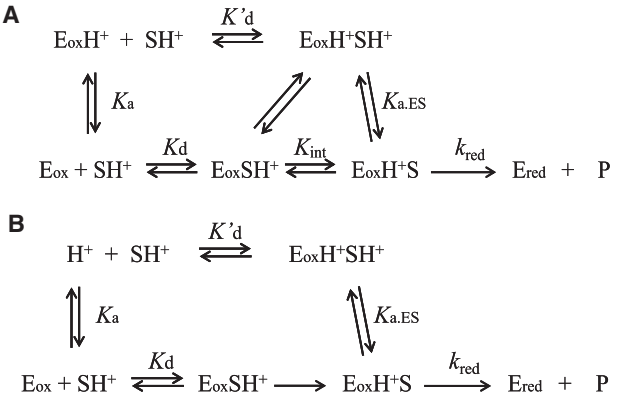

Scheme 2 Control of FAD reduction by ionization of the substrate and enzyme. (A) Generalized mechanism. K_{int} is defined as $K_{int} = [EoxH^+S]/[EoxSH^+]$, and $EoxSH^+$ changes to $EoxH^+S$ by the proton transfer from the amine nitrogen to the ε-amino group of βK358 residue in the active site. The guanidinium moiety of βR69 is assumed to be charged under the experimental conditions, thus the ionization state of the residue is not represented. (B) Proposed mechanism. Symbols are as in A. The conversion of $EoxSH^+$ to $EoxH^+S$ is an irreversible and rapid process.

The pH profile of $k_{red/max}/K_d$ showed a sigmoidal curve and gave one pK_a value (7.1 ± 0.1) for both H-Sar and D-Sar, indicating deprotonation of an ionisable group in the free enzyme or free substrate. The pK_a of sarcosine is approximately 10 (*5*) (Supplementary Table S1), and thus, deprotonation of free sarcosine is not conceivable. As the pK_a of the ε-amino group of Lys358 was reported to be 6.7 (*27*), deprotonation of Lys358 is a possible candidate for the ionization. As described earlier, the active site of SO-U96 is hydrophobic; therefore, the pK_a of Lys358 showed an acid shift, similar to previously reported enzymes (*23*). Contrary to the ionization state of the Lys residue, Arg residues at the 25 internal positions of staphylococcal nuclease are charged at pH 10 and below (*28*). The guanidinium moiety of the Arg side chain is neutralized through multiple hydrogen bonds to polar atoms of the protein and to bound water molecules (*28*). Although we do not know how the guanidinium moiety of Arg69 interacts with the nearby amino acid residues of the oxidized form of SO-U96 without a ligand at the active site, we assume that the Arg69 residue is charged. The carboxylate anion of sarcosine probably interacts with the side chains of Lys358 and Arg69 in the β-subunit as these residues are bound to the carboxylate anion of the substrate analogues MTA and pyrrole 2-carboxylate (*10*).

Under suboptimal acidic conditions, the side chains of both Arg69 and Lys358 are protonated, and side chains are bound to the carboxylate group of sarcosine ($EoxH^+SH^+$). Sarcosine may be deprotonated by the network of hydrogen bonds to the outside of the enzyme (*10*). Under optimum pH conditions, the ε-amino group of Lys358 is deprotonated, but the guanidinium moiety of Arg69 is protonated. Sarcosine is protonated at approximately pH 10 and lower. Therefore, Eox binds with SH^+ to form the $EoxSH^+$ complex (inactive form). To convert the $EoxSH^+$ form to the active $EoxH^+S$ form, we propose a mechanism that differs from that described earlier. The proton on the amine nitrogen moves to the nitrogen atom of βLys358 via the carboxylate group of sarcosine to form the $EoxH^+S$ complex (active form). To verify the mechanism, we constructed the structure of the enzyme–sarcosine complex. The SO-U96 crystal was reduced when the crystal was soaked in a solution containing sarcosine (*10*). Therefore, we could not determine the structure of the sarcosine-bound form of SO-U96. MTA contains an S atom in place of the N atom in sarcosine. Therefore, we matched the structure of MTA bound to SO-U96 and that of free sarcosine (pdb code: YIHHON) (*29*) using the software Chimera (*30*). Figure 5 shows the structure of sarcosine in the active site. As shown in Fig. 5A and B, the distance (2.7–3.6 Å) between the N atom of the amine group of sarcosine and the O atom of the carboxylate and that (2.6–3.8 Å) between the O atom of the carboxylate and the N atom of Lys358 are sufficient lengths for proton transfer to occur. However, direct transfer from the amine N to the Lys N appears not to be possible as the distance (4.7 Å) is rather long. It was

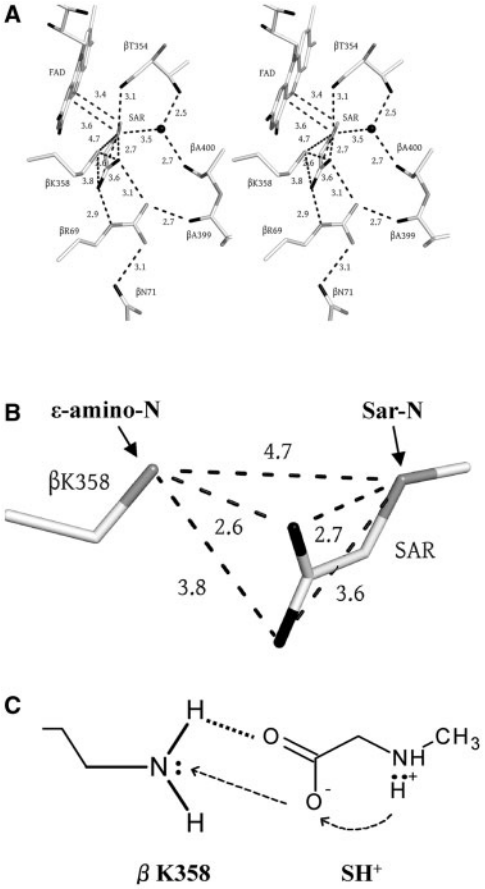

Fig. 5 Structure around sarcosine at the active site of SO-U96 and proton transfer in the active site. (A) The MTA structure in the SO-U96–MTA complex (pdb code: 3ad7) was matched with the sarcosine structure, and the structure around sarcosine (SAR) was generated using the program PyMOL (http://www.pymol.org). The dashed line represents the bond between two atoms, and the number near the line denotes the bond length (Å) between two atoms. (B) Close-up view of sarcosine and the side chain of βK358 in (A). In (A) and (B), water, black sphere; carbon, white; nitrogen, grey; oxygen, black. (C) The predicted proton transfer pathway in the active site is shown.

previously unknown why the Lys358 residue has a low pK_a value in the active site. Our proposed mechanism includes a new role for this residue. It is preferable to include the equilibrium between $EoxSH^+$ and $EoxH^+S$ in Scheme 2A. Applying Equation (1) to Scheme 2A results in the following equation:

$$k_{red/max} = \frac{k_{red/max/ind}}{\{K_{int}/(1+K_{int})\}([H^+]/K_{a,ES})+1} \quad (4)$$

If K_{int} is large, Equation (4) is reduced to:

$$k_{red/max} = \frac{k_{red/max/ind}}{[H^+]/K_{a,ES}+1} \quad (5)$$

and the pK_a value obtained from the $k_{red/max} \sim$ pH profile reflects p$K_{a.ES}$, the secondary amine group of the enzyme-bound sarcosine. In contrast, if K_{int} is small, Equation (4) becomes:

$$k_{red/max} = \frac{k_{red/max/ind}}{(K_{int}/K_{a,ES})[H^+]+1} \quad (6)$$

Because $K_{a,ES}/K_{int}$ is equal to the dissociation constant for $EoxH^+SH^+$ to form $EoxSH^+$ and H^+ in Scheme 2A, the pK_a value obtained from the $k_{red/max} \sim$pH profile reflects the pK_a of an ionisable group of the enzyme, possibly βK358, in the enzyme–substrate complex. The observation that this pK_a shows a clear isotope effect on the deuteration of the substrate indicates that the former is true. This conclusion is supported by the idea that the conversion of $EoxSH^+$ to $EoxH^+S$ includes the formation of an ion pair, which is stabilized by the electrostatic interaction (Fig. 5C). Moreover, we detected only one complex during the FAD reduction (Fig. 3) (*4*, *9*). These findings suggest that the conversion of $EoxSH^+$ to $EoxH^+S$ is an irreversible and rapid process. Thus, we propose Scheme 2B, a modification of Scheme 2A, to explain the present results.

The pH dependence of the steady-state kinetics was bell shaped (Fig. 1). The steady-state rate is dependent on the rates of the reductive and oxidative half-reactions but is not determined by the rate of the single step (*4*). In this work, the ionisable groups affecting the FAD reduction were determined as described earlier, but the pH dependency of the rate of other steps of the reductive half-reaction was not analysed. Moreover, the pH dependency of the oxidative half-reaction was not studied even though we assumed in this work that the kinetic parameters obtained using an air-saturated buffer reflect the reductive half-reaction. Therefore, the ionisable group responsible for the bell-shaped pH dependency of the steady state could not be determined. However, the ionisable groups (the secondary amine group of sarcosine and the ε-amino group of βLys358) determined in the acidic pH region will be useful for explaining the pH profile of the steady-state rate. Regarding the ionisable group(s) in the alkaline region, two candidate ionisable groups are identifiable. One possibility is the ionisation of Lys171 and/or Lys277 of the β-subunit. These Lys residues locate close to the *re*-side of the isoalloxazine ring of the FMN moiety (*10*), and the side chain of Lys277 locates much closer to the ring than that of Lys171 (*9*, *10*). Using the iodacetamide modification, the pK_a of Lys171 was determined to be 8.5 (*27*). This pK_a value is lower than that determined by the steady-state kinetics (approximately 10) (Table 1), and the mutation of the Lys residue to Arg, Ala and Asp was not fatal for the FMN reduction by the reduced FAD (*9*). The Ala171 in the K171A mutant does not contain a proton on its side chain, and the reduction rate of FMN was ~50% of the wild-type SO-U96. These findings indicate that deprotonation of Lys171 is not involved in the loss of activity in the alkaline region. On the other hand, the Lys277 residue locates near Lys171 at the *re*-side of the FMN ring, but the residue did not react with iodacetamide (*31*). This finding indicates that Lys277 has a higher pK_a than Lys171 and is protonated under the conditions of the iodacetamide modification (pH 8.0). If this is the case, deprotonation of Lys 277 may inhibit the FMN reduction in the alkaline region, as the side chain locates close to the FMN ring. Another possibility is the deprotonation of the guanidinium moiety of Arg69. As described earlier, 25 Arg residues are charged in staphylococcal nuclease at pH 10 and below, and it is, therefore, not conceivable that Arg69 has a pK_a of 10 (Table 1). These considerations indicate that deprotonation of Lys277 may be responsible for the loss of activity in the alkaline region (Fig. 1). However, it is clear that further experiments are required to clarify this hypothesis.

Hydrogen (in the form of proton, hydride and hydrogen atom) transfer reactions play vital roles in various enzymes. In this study, hydride transfer of the methyl C (donor) of sarcosine to the N5 atom (acceptor) of the FAD isoalloxazine ring was analysed, and a possible proton transfer in the active site is proposed as discussed earlier. Since the pioneering work regarding H-tunnelling in yeast alcohol dehydrogenase reactions near room temperature (*32*), H-tunnelling experiments have been reported for various enzymes [see (*33*, *34*) for review]. The C–H bond cleavage of the methyl group of sarcosine by SO of *Arthrobacter* sp. 1-IN was reported to be due to vibrationally enhanced ground-state tunnelling (*5*, *35*). We confirmed the H-tunnelling data for SO-U96 (Supplementary Figure S1). As proposed for the H-tunnelling of other enzymes (*36–39*), conformational changes in the active site may modulate the donor-acceptor distance and its dynamics to efficiently tunnel the hydride in the SO-U96-catalysed reaction. As for the proposed proton transfer from the amine N of sarcosine to the ε-amino N of Lys385, it is not known whether this occurs by a quantum proton tunnel.

Conclusion

This study showed that, based on the KIE on enzyme reduction at various pH values, the anionic form of sarcosine is the substrate that is dehydrogenated. Moreover, the results of this study suggest that the ε-amino group of Lys358 of the β-subunit is in the unprotonated form in the active site, which receives the amine proton of sarcosine to be deprotonated.

Supplementary Data

Supplementary Data are available at *JB* Online.

Acknowledgements

The authors thank Prof. Y. Nishina of the Faculty of Life Sciences, Kumamoto University, for critical reading of the manuscript, Prof. K. Sugawara (Department of Physics, School of Science, Kitasato University) for collecting the pdb file of sarcosine and Mr. K. Ujigami for providing technical assistance.

Conflict of interest

None declared.

References

1. Suzuki, H. (1994) Sarcosine oxidase: structure, function, and the application to creatinine determination. *Amino Acids* **7**, 27–43

2. Suzuki, M. (1981) Purification and some properties of sarcosine oxidase from *Corynebacterium* sp. U-96. *J. Biochem.* **89**, 599–607
3. Jorns, M.S. (1985) Properties and catalytic function of the two nonequivalent flavins in sarcosine oxidase. *Biochemistry* **24**, 3189–3194
4. Kawamura-Konishi, Y. and Suzuki, H. (1987) Kinetic studies on the reaction mechanism of sarcosine oxidase. *Biochim. Biophys. Acta.* **915**, 346–356
5. Harris, R.J., Meskys, R., Sutcliffe, M.J., and Scrutton, N.S. (2000) Kinetic studies of the mechanism of carbon–hydrogen bond breakage by the heterotetrameric sarcosine oxidase of *Arthrobacter* sp. 1-IN. *Biochemistry* **39**, 1189–1198
6. Suzuki, H., Tamamura, R., Yajima, S., Kanno, M., and Suguro, M. (2005) *Corynebacterium* sp. U-96 contains a cluster of genes of enzymes for the catabolism of sarcosine to pyruvate. *Biosci. Biotechnol. Biochem.* **69**, 952–956
7. Ida, K., Moriguchi, T., and Suzuki, H. (2005) Crystal structure of heterotetrameric sarcosine oxidase from *Corynebacterium* sp. U-96. *Biochem. Biophys. Res. Commun.* **333**, 359–366
8. Ali, S.N., Zeller, H.-D., Calisto, M.K., and Jorns, M.S. (1991) Kinetics of electron entry, exit, and interflavin electron transfer during catalysis by sarcosine oxidase. *Biochemistry* **30**, 10980–10986
9. Saito, M., Kanno, M., Iizuka, H., and Suzuki, H. (2007) Kinetic studies on the role of Lys-171 and Lys-358 in the β subunit of sarcosine oxidase from *Corynebacterium* sp. U-96. *J. Biochem.* **141**, 799–815
10. Moriguchi, T., Ida, K., Hikima, T., Ueno, G., Yamamoto, M., and Suzuki, H. (2010) Channeling and conformational changes in the heterotetrameric sarcosine oxidase from *Corynebacterium* sp. U-96. *J. Biochem.* **148**, 491–505
11. Bary, Y., Gilboa, H., and Halevi, E. A. (1979) Secondary hydrogen isotope effects. Part 5. Acid and base strengths: corrigendum and addendum. *J. Chem. Soc., Perkin Trans.* **2**, 938–942
12. Pehk, T., Kiirend, E., Lippmaa, E., Ragnarsson, U., and Grehn, L. (1997) Determination of isotope effects on acid–base equilibria by ^{13}C NMR spectroscopy. *J. Chem. Soc., Perkin Trans.* **2**, 445–450
13. Perrin, C. L., Ohta, B. K., Kuperman, J., Liberman, J., and Erdélyi, M. (2005) Stereochemistry of β-deuterium isotope effects on amine basicity. *J. Am. Chem. Soc.* **127**, 9641–9647
14. Basran, J., Sutcliffe, M.J., and Scrutton, N.S. (2001) Deuterium isotope effects during carbon–hydrogen bond cleavage by trimethylamine dehydrogenase. Implications for mechanism and vibrationally assisted hydrogen tunneling in wild-type and mutant enzymes. *J. Biol. Chem.* **276**, 24581–24587
15. Dunn, R.V., Marshall, K.R., Munro, A.W., and Scrutton, N.S. (2008) The pH dependence of kinetic isotope effects in monoamine oxidase A indicates stabilization of the neutral amine in the enzyme–substrate complex. *FEBS J.* **275**, 3850–3858
16. Zhao, G. and Jorns, M.S. (2002) Monomeric sarcosine oxidase: Evidence for an ionizable group in the E·S complex. *Biochemistry* **41**, 9747–9750
17. Zhao, G. and Jorns, M.S. (2005) Ionization of zwitterionic amine substrates bound to monomeric sarcosine oxidase. *Biochemistry* **44**, 16866–16874
18. Zhao, G. and Jorns, M.S. (2006) Spectral and kinetic characterization of the Michaelis charge transfer complex in monomeric sarcosine oxidase. *Biochemistry* **45**, 5985–5992
19. Chen, Z.-W., Hassan-Abdulah, A., Zhao, G., Jorns, M.S., and Mathews, F.S. (2006) Heterotetrameric sarcosine oxidase: structure of a diflavin metalloenzyme at 1.85 Å resolution. *J. Mol. Biol.* **360**, 1000–1018
20. Trickey, P., Wagner, M.A., Jorns, M.S., and Mathews, F.S. (1999) Monomeric sarcosine oxidase: structure of a covalently flavinylated amine oxidizing enzyme. *Structure* **7**, 331–345
21. Massey, V., Müller, F., Feldberg, R., Schuman, M., Sullivan, P.A., Howell, L.G., Mayhew, S.G., Matthews, R.G., and Foust, G.P. (1969) The reactivity of flavoproteins with sulfite. Possible relevance to the problem of oxygen reactivity. *J. Biol. Chem.* **244**, 3999–4006
22. Royo, M. and Fitzpatrick, P. F. (2005) Mechanistic studies of mouse polyamine oxidase with N1, N12-bisethylspermine as a substrate. *Biochemistry* **44**, 7079–7084
23. Harris, T.K. and Turner, G.J. (2002) Structural basis of perturbed p*K*a values of catalytic groups in enzyme active sites. IUBMB. *Life* **53**, 85–98
24. Stites, W.E., Gittis, A.G., Lattman, E.E., and Shortle, D. (1991) In a staphylococcal nuclease mutant the side-chain of a lysine replacing valine 66 is fully buried in the hydrophobic core. *J. Mol. Biol.* **221**, 7–14
25. Dwyer, J.J., Gittis, A.G., Karp, D.A., Lattman, E.E., Spencer, D.S., Stites, W.E., and García-Moreno, E.B. (2000) High apparent dielectric constants in the interior of a protein reflect water penetration. *Biophys. J.* **79**, 16101620
26. Basran, J., Sutcliffe, M.J., and Scrutton, N.S. (2001) Optimizing the Michaelis complex of trimethylamine dehydrogenase. Identification of interactions that perturb the ionization of substrate and facilitate catalysis with trimethylamine base. *J. Biol. Chem.* **276**, 42887–42892
27. Mukouyama, E.B., Oguchi, M., Kodera, Y., Maeda, T., and Suzuki, H. (2004) Low p*K*a lysine residues at the active site of sarcosine oxidase from *Corynebacterium* sp.U-96. *Biochem. Biophys. Res. Commun.* **320**, 846–851
28. Harms, M.J., Schlessman, J.L., Sue, G.R., and García-Moreno, E.B. (2011) Arginine residues at internal positions in a protein are always charged. *Proc. Natl. Acad. Sci. USA* **108**, 18954–18959
29. Dittrich, B. and Spackman, M. A. (2007) Can the interaction density be measured? The example of the non-standard amino acid sarcosine. *Acta Cryst.* **A63**, 426–436
30. Huang, C.C., Couch, G.S., Pettersen, E.F., and Ferrin, T.E. (1996) Chimera: an extensible molecular modeling application constructed using standard components. *Pacific Symp. Biocomput.* **1**, 724
31. Suzuki, H. and Kawamura-Konishi, Y. (1991) Cysteine residues in the active site of *Corynebacterium* sarcosine oxidase. *J. Biochem.* **109**, 909–917
32. Cha, Y., Murray, C.J., and Klinman, J.P. (1989) Hydrogen tunneling in enzyme reactions. *Science* **243**, 1325–1330
33. Scrutton, N.S., Basran, J., and Sutcliffe, M.J. (1999) New insights into enzyme catalysis. Ground state tunneling driven by protein dynamics. *Eur. J. Biochem.* **264**, 666–671

34. Liang, Z.-X. and Klinman, J.P. (2004) Structural bases of hydrogen tunneling in enzymes: progress and puzzles. *Curr. Opin. Struc. Biol.* **14**, 648–655
35. Basran, J., Sutcliffe, M.J., and Scrutton, N.S. (1999) Enzymatic H-transfer requires vibration-driven extreme tunneling. *Biochemistry* **38**, 3218–3222
36. Pudney, C. R., Hay, S., Levy, C., Pang, J., Sutcliffe, M. J., Leys, D., and Scrutton, N. S. (2009) Evidence to support the hypothesis that promoting vibrations enhance the rate of an enzyme catalyzed H-tunneling reaction *J. Am. Chem. Soc.* **131**, 17072–17073
37. Loveridge, E.J., Tey, L.-H., and Allemann, R.K. (2010) Solvent effects on catalysis by *Escherichia coli* dihydrofolate reductase. *J. Am. Chem. Soc.* **132**, 1137–1143
38. Pudney, C.R., Johannissen, L.O., Sutcliffe, M.J., Hay, S., and Scrutton, N.S. (2010) Direct analysis of donor-acceptor distance and relationship to isotope effects and the force constant for barrier compression in enzymatic H-tunneling reactions. *J. Am. Chem. Soc.* **132**, 11329–11335
39. Stojković, V., Laura, L., Perissinotti, L.L., Willmer, D., Benkovic, S.J., and Kohen, A. (2012) Effects of the donor-acceptor distance and dynamics on hydride tunneling in the dihydrofolate reductase catalyzed reaction. *J. Am. Chem. Soc.* **134**, 1738–1745